Ammonia Borane Dehydrogenation Promoted by a Pincer-Square-Planar Rhodium(I)-Monohydride: A Stepwise Hydrogen Transfer from the Substrate to the Catalyst

Miguel A. Esteruelas,[‡,]* Pau Nolis,[#] Montserrat Oliván,[‡] Enrique Oñate,[‡] Adelina Vallribera,[†] and Andrea Vélez[‡]

[‡] Departamento de Química Inorgánica, Instituto de Síntesis Química y Catálisis Homogénea (ISQCH), Centro de Innovación en Química Avanzada (ORFEO-CINQA), Universidad de Zaragoza - CSIC, 50009 Zaragoza, Spain

[#] Servei de Ressonància Magnètica Nuclear and Departament de Química, Universitat Autònoma de Barcelona, Campus UAB, 08193 Cerdanyola del Vallès, Barcelona, Spain

[†] Department de Química, Centro de Innovación en Química Avanzada (ORFEO-CINQA), Universitat Autònoma de Barcelona, Campus UAB, 08193 Cerdanyola del Vallès, Barcelona, Spain

KEYWORDS: ammonia-borane dehydrogenation, rhodium, hydride, DFT, mechanism.

ABSTRACT: The pincer d^8-monohydride complex RhH{xant(P^iPr_2)$_2$} (xant(P^iPr_2)$_2$ = 9,9-dimethyl-4,5-bis(diisopropylphosphino)xanthene) promotes the release of 1 equiv of hydrogen from H_3BNH_3 and H_3BNHMe_2 with $TOF_{50\%}$ values of 3150 h^{-1} and 1725 h^{-1}, to afford $[BH_2NH_2]_n$ and $[BH_2NMe_2]_2$, and the tandem ammonia-borane dehydrogenation – cyclohexene hydrogenation. DFT calculations on the ammonia-borane dehydrogenation suggest that the process takes place by means of *cis*-κ^2-PP-species, through four stages including: i) Shimoi type coordination of ammonia-borane, ii) homolytic addition of the coordinated H-B bond to afford a five-coordinate-dihydride-boryl-rhodium(III) intermediate, iii) reductive-intramolecular proton transfer from the NH_3 group to one of the hydride ligands, and iv) release of H_2 from the resulting square-planar hydride-dihydrogen-rhodium(I) intermediate.

INTRODUCTION

Ammonia-borane is a promising chemical hydrogen storage material due to its high hydrogen content[1] and the fact that a variety of transition metal compounds have the ability of promoting its kinetically controlled dehydrogenation, including complexes of Fe,[2] Ru,[3] Os,[4] Co,[5] Rh,[6] Ir,[7] Ni,[8] and Pd.[9]

Inner- and outer-sphere mechanisms have been generally considered in order to rationalize the dehydrogenation (Scheme 1).[10] In both cases, the formation of a dihydrogen intermediate is proposed to be the key step of the process. The inner-sphere mechanism (a) is characterized by a change of two units in the metal oxidation state, involving a dihydride-dihydrogen tautomerization. The dihydride is formed by hydrogen transfer from ammonia-borane to the catalyst metal center. This transfer can be concerted (a_1) or stepwise (a_2). While the first of them directly affords the dihydride,[11] the second one takes place via an stabilized boryl intermediate which undergoes a β-hydrogen elimination reaction.[12] The oxidation state of the catalyst metal center does not change during the outer-sphere catalysis (b), which avoids the dihydride intermediate. In contrast to the inner-sphere process, the formation of the dihydrogen intermediate is assisted by a ligand of the bifunctional catalyst.[13] There is a third mechanism (c), which operates for dihydride catalysts and has been observed for the dehydrogenation promoted by the d^6-species IrH_2(POCOP^{t}Bu) (POCOP^{t}Bu = 1,3-(OP^{t}Bu$_2$)$_2$C$_6$H$_3$)[14] and $OsH_2(CO)(P^iPr_3)_2$.[15] In this dihydride route, the reactions take place via dihydride-dihydrogen intermediates which result from the concerted BH-hydride and NH-proton transfers from ammonia-borane to the metal center and a hydride ligand, respectively, without any change in the metal oxidation state nor ligand assistance.

We have now found DFT evidence for the existence of a monohydride pathway for the ammonia-borane dehydrogenation, which involves a stepwise hydrogen transfer from the substrate to the metal center, and produces a change of two units in the metal oxidation state.

RESULTS AND DISCUSSION

Dehydrogenation of Ammonia-borane and Dimethylamineborane. The d^8-complex RhH{xant(P^iPr_2)$_2$} (**1**; xant(P^iPr_2)$_2$ = 9,9-dimethyl-4,5-bis(diisopropylphosphino)xanthene) is a notable square-planar rhodium(I)-monohydride.[16] This compound activates B-H, C-H and Si-H bonds to afford d^8-square planar boryl-, aryl-, and silyl-derivatives.[17] The boryl- and aryl-species are key intermediates for the direct borylation of aromatic compounds[18] and for the decyanative borylation of nitriles.[19] In agreement with the ability of **1** to activate B-H bonds, it promotes the release of 1 mol of molecular hydrogen per mole of substrate from ammonia-borane (eq 1) and dimethylamine-borane (eq 2), with turnover frequency values at 50% conversion ($TOF_{50\%}$) of 3150 h^{-1} and 1725 h^{-1}, respectively, in tetrahydrofuran as solvent at 31 ºC. Figure 1 shows

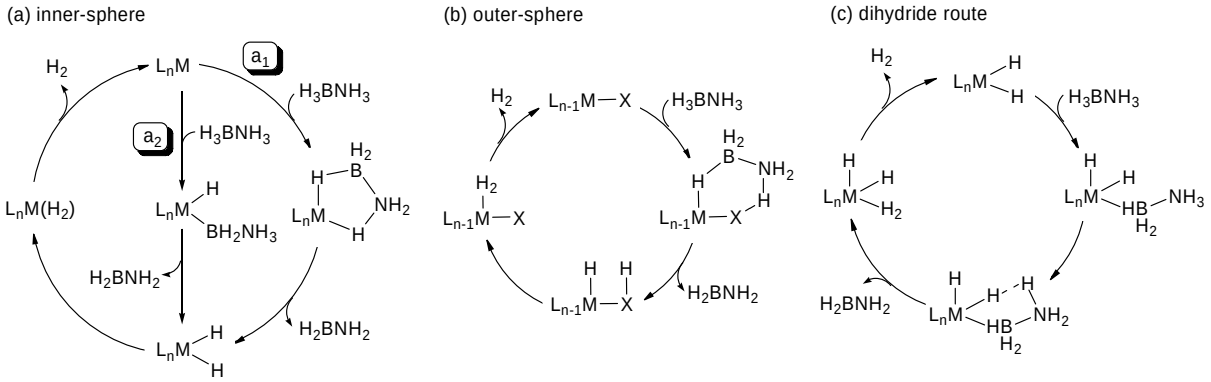

Scheme 1. Mechanistic proposals for the catalytic ammonia-borane dehydrogenation.

the course of the dehydrogenation of ammonia-borane, which yields polyaminoborane according to the IR and $^{11}B\{^1H\}$ and ^{11}B-MQMAS[20] solid state NMR spectra of the formed white insoluble material. The ^{11}B NMR spectrum of the solution at the end of the dimethylamineborane dehydrogenation process contains at 4.9 ppm the characteristic triplet (J_{B-H} = 113 Hz) corresponding to the dimer $[H_2BNMe_2]_2$. No traces of the linear diborazane $H_3B\text{-}NMe_2\text{-}BH_2\text{-}NHMe_2$ were observed at any point of the reaction, which suggests an off-metal dimerization of $H_2B{=}NMe_2$.[21]

$$n\ H_3BNH_3 \xrightarrow[\text{THF, 31 ºC}]{\mathbf{1}\ (1\ mol\%)} n\ H_2\uparrow + [NH_2BH_2]_n \quad (1)$$

$$H_3BNHMe_2 \xrightarrow[\text{THF, 31 ºC}]{\mathbf{1}\ (1\ mol\%)} H_2\uparrow + 1/2\ [H_2BNMe_2]_2 \quad (2)$$

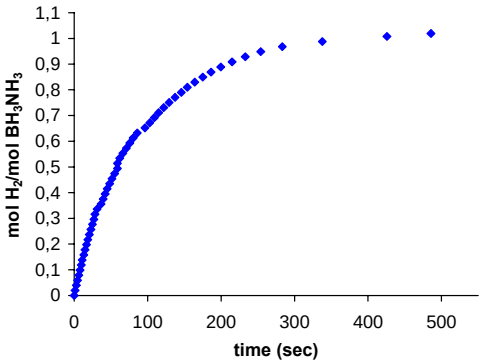

Figure 1. H_2 evolution in the catalytic de hydrogenation of BH_3NH_3 with **1** (1 mol %) in THF at 31 ºC.

Figure 2A shows the $^{11}B\{^1H\}$ and ^{11}B-MQMAS NMR spectra of the white material obtained in the dehydrocoupling of ammonia-borane. The ^{11}B-MQMAS spectrum reveals that the peak centered at -10.21 ppm in the $^{11}B\{^1H\}$ NMR spectrum is split into three signals (A, B, and C) along the F1(TQ) axis, which is consistent with three different chemical environments. Signals A and B were assigned to $–BH_2–$ units on the basis of their δ_{iso} values (-11.02 and -8.51, respectively), which compare well with the DFT/GIAO chemical shifts calculated by Sneddon and co-workers for materials of this type.[22] Signal C was assigned to branching –BH– groups because of its δ_{iso} value of -5.35 agrees well with that theoretically predicted, -5.90. Although the integration values 10.1% (A), 83.6% (B) and 6.3 % (C) should be taken carefully, because inherently MQMAS is not a quantitative experiment, they suggest that the amount of branched polymer in the sample is low. In this context, it should be noted that the A:C integration ratio is about 2. This seems to indicate that both units belong to the same branch. Other noticeable feature of the spectra is the absence, at about -20 ppm, of any observable signal corresponding to terminal BH_3 units, which is consistent with a very long chained polymer. The $^{11}B\{^1H\}$ and ^{11}B-MQMAS NMR spectra of the material obtained from the dehydrogenation of ammonia-borane promoted by the osmium dihydride $OsH_2(CO)(P^iPr_3)_2$ (Figure 2B) are similar, although the integrations (6.8% (A), 89.2 (B) and 3.9% (C)) suggest a lower number of branches in the material and the presence of a signal centered at -19.60 (terminal BH_3 units) indicates a shorter linear polymer.

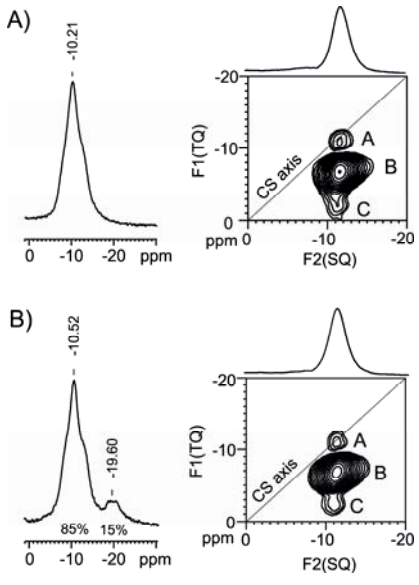

Figure 2. $^{11}B\{^1H\}$ and ^{11}B-MQMAS NMR spectra of polyaminoborane obtained from the dehydrogenation of ammonia-borane promoted by $RhH\{xant(P^iPr_2)_2\}$ (A) and $OsH_2(CO)(P^iPr_3)_2$ (B).

Tandem Ammonia-borane Dehydrogenation – Cyclohexene Hydrogenation. The presence of cyclohexene in the catalytic solution does not modify the dehydrocoupling. A 1:1 ammonia-borane : cyclohexene mixture initially undergoes the selective dehydrocoupling of ammonia-borane and subsequently the generated molecular hydrogen reduces the olefin with a $TOF_{50\%}$ value of 12 h^{-1}. During the tandem process (Scheme 2), no formation of any borylation product is observed. This is consistent with the release of H_2BNH_2, which experiences polymerization out the coordination sphere of the metal, initiated by a nucleophile.[23]

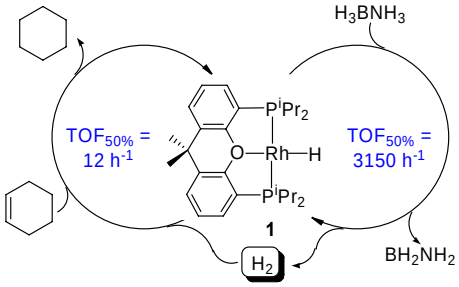

Scheme 2. Tandem ammonia-borane dehydrogenation – cyclohexene hydrogenation.

Attempts to detect intermediate metallic species during the dehydrogenation process were unsuccessful. Between 20 ºC and -80 ºC, in toluene-d_8, the ^{1}H NMR spectrum of **1** in the presence of ammonia-borane is identical to the spectrum of **1** under 1 atm of molecular hydrogen (Figure 3). At 20 ºC, the spectrum contains a broad signal centered at about -13 ppm, which decoalesces between 20 ºC and 0ºC to afford two signals centered at -11.1 and -21.3 ppm, with a 4:1 integrated intensity ratio. At temperatures lower than -50 ºC, these signals undergo subsequent decoalescence. Thus, at -80 ºC a complex and poorly informative spectrum is observed. This behavior suggest that once the dehydrogenation is finished, the resting state of the system is a dynamic equilibrium between $RhH_5\{xant(P^iPr_2)_2\}$ (**2**) species,[24] containing a bidentate diphosphine to respect the 18 electron rule, which also act as precatalyst for the cyclohexene reduction. DFT calculations (energies calculated at the M06//6-311G(d,p)/SDD level, using structures optimized on the M06//6-31G(d,p)/lanl2dz level) reveal that there are three low energy $RhH_5\{xant(P^iPr_2)_2\}$ structures differing by 8.5 kcal·mol^{-1} (ΔG, toluene, 298 K), among all possible RhH_5 stoichiometries. They show nonclassical interaction between the coordinated hydrogen atoms[25] and contain a *cis*-k^2-PP-diphosphine (Chart 1): the *fac*-trihydride-dihydrogen **2a** (0 kcal·mol^{-1}; d_{H2} = 0.816 Å) and the five-coordinate-rhodium(I) hydride-bis(dihydrogen) derivatives **2b** (3.4 kcal·mol^{-1}; d_{H2} = 0.826 and 0.842 Å) and **2c** (8.3 kcal·mol^{-1}; d_{H2} = 0.842 and 0.870 Å). Under vacuum, complex **1** is regenerated.

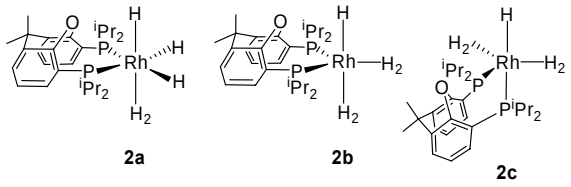

Chart 1. Optimized structures for $RhH_5\{xant(P^iPr_2)_2\}$ (**2**).

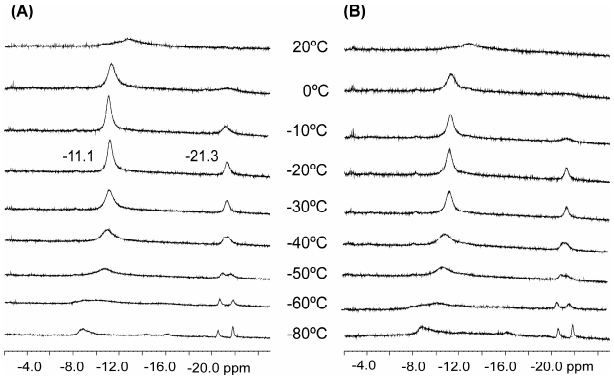

Figure 3. ^{1}H NMR spectra as a function of temperature (400 MHz, toluene-d_8, high field region) of the solutions resulting from the reaction of $RhH\{xant(P^iPr_2)_2\}$ (**1**) with BH_3NH_3 (A) and from the exposure of $RhH\{xant(P^iPr_2)_2\}$ (**1**) to a hydrogen atmosphere (B).

Mechanism of the Ammonia-borane Dehydrogenation. To gain insight the mechanism of the dehydrogenation of ammonia-borane, we have carried out DFT calculations. The changes in free energy (ΔG) have been computed in tetrahydrofuran at 304 K. Figure 4 shows the obtained energy profile, Scheme 3 summarizes the steps of the process, and Chart 2 collects the transition states.[26]

Complex **1** initially dissociates the oxygen atom of the diphosphine to afford the tricoordinated T-shaped intermediate **3**. The dissociation occurs through the transition state **TS(1-3)**, with an activation energy of 17.3 kcal·mol^{-1}, and destabilizes the system by 12.6 kcal·mol^{-1}. The subsequent coordination of ammonia-borane to **3** in a Shimoi manner[27] leads to the square-planar intermediate **4**. The reaction is exothermic by 1.7 kcal·mol^{-1}. *Cis*-κ^2-PP-xantphos-rhodium(I) complexes coordinating amine-boranes have been previously isolated and fully characterized by Weller and co-workers.[28] The metal center of **4** homolytically adds the coordinated B-H bond, overcoming an activation barrier of 11.1 kcal·mol^{-1}, to afford the dihydride **5**, which contains a stabilized boryl ligand. The oxidative addition takes place via the transition state **TS(4-5)**, which can be described as a σ-borane species with Rh-H, H-B, and Rh-B distances of 1.598 Å, 1.796 Å, and 2.212 Å, respectively. The five-coordinate-rodium(III) complex **5**[29] evolves into the hydride-dihydrogen **6** by means of a reductive intramolecular proton transfer from the NH_3 group to one of the hydride ligands. The transfer, which has an activation energy of 13.9 kcal·mol^{-1} (31.7 kcal·mol^{-1} with regard to **1** + H_3BNH_3)[30] is the determining step of the dehydrogenation and takes place through **TS(5-6)**. This transition state can be described as a η^1-H_2 species, where the asymmetric dihydrogen (d_{H-H} = 1.023 Å) is stabilized by interaction with the NH_2 group of the boron ligand (d_{H-N} = 1.400 Å). The hydride-dihydrogen intermediate **6** is also a square-planar species with the dihydrogen ligand (d_{H-H} = 0.840 Å) bent with regard to the coordination plane. The release of the dihydrogen ligand regenerates **3** and affords 2.1 kcal·mol^{-1}. At the end of the catalysis, the coordination of two hydrogen molecules from the generated hydrogen atmosphere yields the resting species **2**. Under the catalytic conditions the energies of **2a**, **2b**, and **2c** are 6.5, 11.7 and 16.7 kcal·mol^{-1}, re-

spectively; i.e. they are less stable than **1** + $\mathbf{BH_3NH_3}$, but lie below **TS(5-6)**.

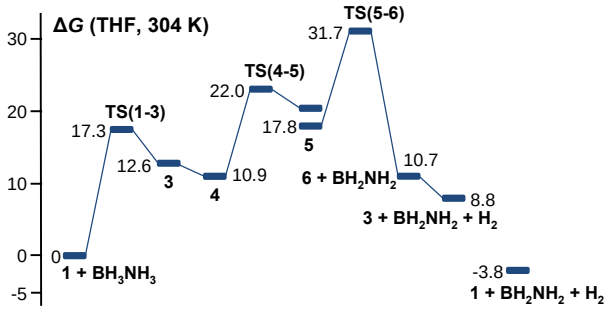

Figure 4. Energy profile (ΔG in kcal·mol^{-1}) for BH_3NH_3 dehydrogenation. The energy of **1** + $\mathbf{BH_3NH_3}$ has been taken as reference.

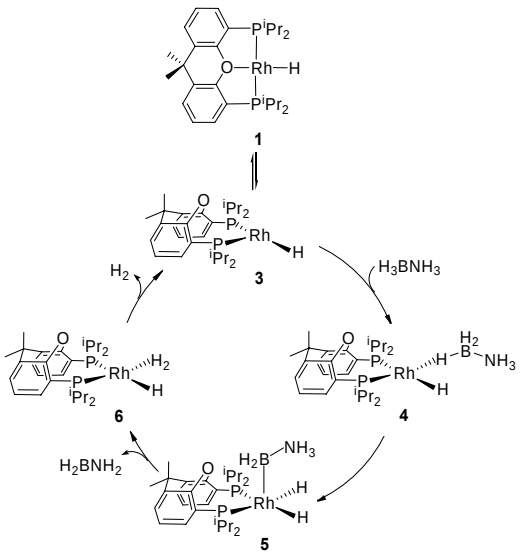

Scheme 3. Mechanistic proposal.

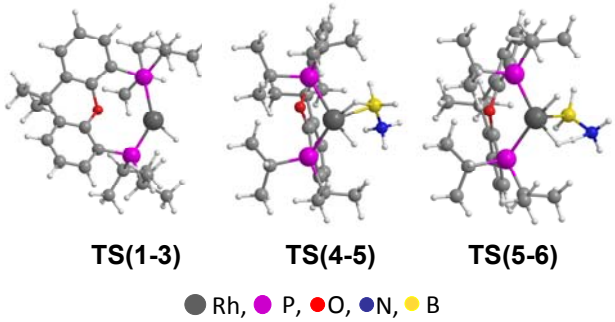

Chart 2. Optimized structures of **TS(1-3)**, **TS(4-5)** and **TS(5-6)**.

CONCLUSION

The d^8-monohydride complex RhH{xant(P^iPr_2)$_2$} promotes the release of 1 equiv of molecular hydrogen from ammonia-borane and dimethylamine-borane and a ammonia-borane dehydrogenation - cyclohexene hydrogenation tandem process. At the end of the dehydrocoupling an equilibrium between novel RhH_5{xant(P^iPr_2)$_2$} species is formed. They show nonclassical interaction between the coordinated hydrogen atoms and contain a *cis*-κ^2-PP-diphosphine. DFT calculations reveal that, in contrast to the previously reported dihydride route, in this monohydride pathway the ammonia-borane dehydrogenation takes place via stepwise hydrogen transfer from the substrate to the catalyst, through a five-coordinate dihydride-boryl-rhodium(III) intermediate where the diphosphine acts as *cis*-κ^2-PP-chelate.

EXPERIMENTAL SECTION

General Information. All manipulations were performed with rigorous exclusion of air at an argon/vacuum manifold using standard Schlenk-tube techniques or in a dry-box (MB-UNILAB). Solvents were dried by the usual procedures and distilled under argon prior to use or obtained oxygen- and water-free from an MBraun solvent purification apparatus. ^{1}H, ^{31}P{^{1}H}, ^{11}B and ^{11}B{^{1}H} NMR spectra were recorded on Bruker 300 ARX, Bruker Avance 300 MHz or Bruker Avance 400 MHz instruments. Solid state ^{11}B and ^{11}B MQMAS experiments were performed on a BRUKER Avance III at a magnetic field of 9.4 T equipped with a double channel 4.0 mm MAS probe. Sample spinning was set to 14 KHz in all experiments. The ^{11}B MQMAS was acquired using the mp3qzqf pulse program of Bruker library. Size of FID was acquired with 2K(TD2) x 32(TD1) and processing using the *xfshear* macro provided by Bruker and STATES-TPPI protocol with zero-filling in both dimension. Chemical shifts (expressed in parts per million) are referenced to residual solvent peaks (^{1}H), external 85% H_3PO_4 (^{31}P{^{1}H}) or BF_3·OEt_2 (^{11}B). Coupling constants are given in hertz. Attenuated total reflection infrared spectra (ATR-IR) of solid samples were run on a Perkin-Elmer Spectrum 100 FT-IR spectrometer. BH_3NH_3 and BH_3NHMe_2 were purchased from commercial sources and used without further purification. RhH{xant(P^iPr_2)$_2$} (**1**) was prepared according to the published method.[16]

Catalytic Dehydrogenations

BH_3NH_3. Under argon, 200 µL of a THF solution of complex **1** (10.9 mg, 0.02 mmol) was added via syringe to a 5 mL solution of BH_3NH_3 (61.8 mg, 2 mmol) placed into a 25 mL flask attached to a gas burette and immersed in a 31 ºC bath, and the mixture was vigorously shaken (500 rpm) during the run. The reaction was monitored by measuring the volume of evolved hydrogen with time until hydrogen evolution stopped. During the reaction a white solid was formed which was separated by decantation, washed with THF (8 x 1 mL) and diethyl ether (4 x 1 mL), and dried in vacuum. The IR spectrum confirms the presence of polyaminoborane (Figure S1). The assignment of the signals was made by comparison with the data reported by Manners et al.[7b,31] $TOF_{50\%}$ = 3150 h^{-1} (average of four runs).

BH_3NHMe_2. Under argon, 200 µL of a THF solution of complex **1** (10.9 mg, 0.02 mmol) was added via syringe to a 5 mL solution of BH_3NHMe_2 (117.8, 2 mmol) placed into a 25 mL flask attached to a gas burette and immersed in a 31 ºC bath, and the mixture was vigorously shaken (500 rpm) during the run. The reaction was monitored by measuring the volume of evolved hydrogen with time until the hydrogen evolution stopped (Figure S2). The ^{11}B NMR spectrum of the solution after the hydrogen evolution stopped shows a triplet

at 4.87 ppm ($^1J_{B-H}$ = 113 Hz) assigned to $[H_2BNMe_2]_2$ (Figure S3). $TOF_{50\%}$ = 1725 h^{-1} (average of four runs).

Tandem Dehydrogenation of BH_3NH_3 – Hydrogenation of Cyclohexene. Under argon, 200 μL of a THF solution of complex **1** (10.9 mg, 0.02 mmol) and cyclohexene (202 μl, 2 mmol) was added via syringe to a 5 mL solution of BH_3NH_3 (61.8 mg, 2 mmol) placed into a 25 mL flask attached to a gas burette and immersed in a 31 ºC bath, and the mixture was vigorously shaken (500 rpm) during the run. The reaction was monitored by measuring the volume of evolved hydrogen - consumed hydrogen with time (Figure S4). During the reaction a white solid of polyaminoborane was formed. Cyclohexane was identified by a GC-MS experiment run on an Agilent 5973 mass selective detector interfaced to an Agilent 6890 series gas chromatograph system. The sample was injected into a 30 m x 250 μm HP-5MS 5% phenylmethylsiloxane column with a film thickness of 0.17 μm (Agilent). The GC oven temperature was programmed as follows: 35 ºC for 6 min, 35-280 ºC at 25 ºC/min, 280 ºC for 4 min. The carrier gas was helium at a flow of 1 mL/min.

Reaction of RhH{xant(P^iPr_2)$_2$} (1) with BH_3NH_3: Spectroscopic Detection of RhH_5{xant(P^iPr_2)$_2$} species. A screw-top NMR tube containing a solution of **1** (21 mg, 0.038 mmol) in toluene-d_8 (0.4 mL) and cooled at -78 ºC was treated with BH_3NH_3 (2.4 mg, 0.068 mmol), and it was vigorously shaken. Immediately the NMR was introduced in a NMR probe precooled to -60 ºC. Figure 3(A) shows the high field region of the ^{1}H NMR spectra as a function of temperature.

Exposure of RhH{xant(P^iPr_2)$_2$} (1) to a Hydrogen Atmosphere: Spectroscopic Detection of RhH_5{xant(P^iPr_2)$_2$} species. A low pressure/vacuum NMR tube was charged with a solution of **1** in toluene-d_8 (0.5 mL), and the argon atmosphere was replaced by a hydrogen atmosphere (1 atm). Figure 3(B) shows the high field region of the ^{1}H NMR spectra as a function of temperature.

Computational Details. All calculations in the mechanistic studies were performed at the DFT level using the M06[32] functional as implemented in Gaussian09.[33] In geometry optimizations Rh atom was described by means of an effective core potential Lanl2dz for the inner electron and its associated double-ζ basis set for the outer ones. The 6-31G(d,p) basis set was used for the H, C, B, N, O and P atoms. All geometries were fully optimized in THF (ε = 7.4257) at 304 K or in toluene (ε = 2.37) at 298 K (**2a**, **2b** and **2c**) solvents using the continuum SMD model.[34] Energy calculations were performed at the M06//6-311G(d,p)/SDD[35] level in THF at 304 K or in toluene at 298 K (**2a**, **2b** and **2c**) using structures optimized on the M06//6-31G(d,p)/lanl2dz.

Transition states were identified by having one imaginary frequency in the Hessian matrix. It was confirmed that transition states connect with the corresponding intermediates by means of application of an eigenvector corresponding to the imaginary frequency and subsequent optimization of the resulting structures. The complex **5** shown in Figure S6 appears in the energy profile as two rotamers (**5a** and **5b**) by rotation about the Rh-B single bond.

ASSOCIATED CONTENT

Supporting Information. IR spectrum of the polyaminoborane obtained from the catalytic dehydrogenation reaction, plot of the H_2 evolution in the catalytic dehydrogenation of BH_3NHMe_2 with **1** (1 mol %), ^{11}B NMR spectrum of the catalytic dehydrogenation of BH_3NHMe_2 after finishing the hydrogen evolution, plot of the volume of evolved - consumed hydrogen in the tandem dehydrogenation of BH_3NH_3 – hydrogenation of cyclohexene catalyzed by **1**, and computational details. The supplemental file esi-theoretical.xyz contains the computed Cartesian coordinates of the molecules reported in this study. This material is available free of charge via the Internet at http://pubs.acs.org.

AUTHOR INFORMATION

Corresponding Author

* E-mail: maester@unizar.es.

Notes

The authors declare no competing financial interest.

ACKNOWLEDGMENT

Financial support from the MINECO of Spain (Projects CTQ2014-52799-P, CTQ2014-53662-P and CTQ2014-51912-REDC), the Diputación General de Aragón (E-35), the DURSI-Generalitat de Catalunya (2014SGR1105), FEDER, and the European Social Fund is acknowledged.

REFERENCES

(1) (a) Stephens, F. H.; Pons, V.; Baker, R. T. *Dalton Trans.* **2007**, 2613-2626. (b) Hamilton, C. W.; Baker, R. T.; Staubitz, A.; Manners, I. *Chem. Soc. Rev.* **2009**, *38*, 279-293. (c) Smythe, N. C.; Gordon, J. C. *Eur. J. Inorg. Chem.* **2010**, 509-521. (d) Staubitz, A.; Robertson, A. P. M.; Manners, I. *Chem. Rev.* **2010**, *110*, 4079-4124. (e) Yadav, M:, Xu, Q. *Energy Environ. Sci.* **2012**, *5*, 9698-9725. (f) Dalebrook, A. F.; Gan, W.; Grasemann, M.; Moret, S.; Laurenczy, G. *Chem. Commun.* **2013**, *49*, 8735-8751. (g) Li, H.; Yang, Q.; Chen, X.; Shore, S. G. *J. Organomet. Chem.* **2014**, *751*, 60-66.

(2) (a) Vance, J. R.; Robertson, A. P. M.; Lee, K.; Manners, I. *Chem. Eur. J.* **2011**, *17*, 4099-4103. (b) Baker, R. T.; Gordon, J. C.; Hamilton, C. W.; Henson, N. J.; Lin, P.-H.; Maguire, S.; Murugesu, M.; Scott, B. L.; Smythe, N. C. *J. Am. Chem. Soc.* **2012**, *134*, 5598-5609. (c) Sonnenberg, J. F.; Morris, R. H. *ACS Catal.* **2013**, *3*, 1092-1102. (d) Battacharya, P.; Krause, J. A.; Guan, H. *J. Am. Chem. Soc.* **2014**, *136*, 11153-11161.

(3) (a) Blaquiere, N.; Diallo-Garcia, S.; Gorelsky, S. I.; Black, D. A.; Fagnou, K. *J. Am. Chem. Soc.* **2008**, *130*, 14034−14035. (b) Friedrich, A.; Drees, M.; Schneider, S. *Chem. Eur. J.* **2009**, *15*, 10339-10342. (c) Käβ, M.; Friedrich, A.; Drees, M.; Schneider, S. *Angew. Chem. Int. Ed.* **2009**, *48*, 905−907. (d) Conley, B. L.; Guess, D.; Williams, T. J. *J. Am. Chem. Soc.* **2011**, *133*, 14212−14215.

(4) Esteruelas, M. A.; Fernández, I.; López, A. M.; Mora, M.; Oñate, E. *Organometallics* **2014**, *33*, 1104-1107.

(5) Pagano, J. K.; Stelmach, J. P. W.; Waterman, R. *Dalton Trans.* **2015**, *44*, 12074-12077.

(6) (a) Jaska, C. A.; Temple, K.; Lough, A. J.; Manners, I. *Chem. Commun.* **2001**, 962−963. (b) Jaska, C. A.; Temple, K.; Lough, A. J.; Manners, I. *J. Am. Chem. Soc.* **2003**, *125*, 9424−9434. (c) Douglas, T. M.; Chaplin, A. B.; Weller, A. S. *J. Am. Chem. Soc.* **2008**, *130*, 14432-14433.

(7) (a) Denney, M. C.; Pons, V.; Hebden, T. J.; Heinekey, D. M.; Goldberg, K. I. *J. Am. Chem. Soc.* **2006**, *128*, 12048−12049. (b) Staubitz, A.; Presa Soto, A.; Manners, I. *Angew. Chem. Int. Ed.* **2008**, *47*, 6212-6215. (c) Dietrich, B. L.; Goldberg, K. I.; Heinekey, D. M.; Autrey, T.; Linehan, J. C. *Inorg. Chem.* **2008**, *47*, 8583-8585. (d) Kumar, A.; Johnson, H. C.; Hooper, T. N.; Weller, A. S.; Algarra, A. G.; Macgregor, S. A. *Chem. Sci.* **2014**, 5, 2546-2553.

(8) Yang, X.; Hall, M. B. *J. Am. Chem. Soc.* **2008**, *130*, 1798−1799.

(9) (a) Kim, S.-K.; Han, W.-S.; Kim, T.-J.; Kim, T.-Y.; Nam, S. W.; Mitoraj, M.; Piekoś, Ł.; Michalak, A.; Hwang, S.-J.; Kang, S. O. *J. Am. Chem. Soc.* **2010**, *132*, 9954−9955. (b) Rossin, A.; Bottari, G.; Lozano-Vila, A. M.; Paneque, M.; Peruzzini, A.; Rossi, A.; Zanobini, F. *Dalton Trans.* **2013**, *42*, 3533-3541.

(10) Waterman, R. *Chem. Soc. Rev.* **2013**, *42*, 5629-5641

(11) Butera, V.; Russo, N.; Sicilia, E. *ACS Catal.* **2014**, *4*, 1104-1113

(12) Keaton, R. J.; Blacquiere, J. M.; Baker, R. T. *J. Am. Chem. Soc.* **2007**, *129*, 1844-1845.

(13) (a) Conley, B. L.; Williams, T. J. *Chem. Commun.* **2010**, *46*, 4815-4817. (b) Schreiber, D. F.; O'Connor, C.; Grave, C.; Ortin, Y.; Müller-Bunz, H.; Phillips, A. D. *ACS Catal.* **2012**, *2*, 2505-2511. (c) Marziale, A. N.; Friedrich, A.; Klopsch, I.; Drees, M.; Celinski, V. R.; Schmedt auf der Günne, J.; Schneider, S. *J. Am. Chem. Soc.* **2013**, *135*, 13342-13355. (d) Glüer, A.; Förster, M.; Celinski, V. R.; Schmedt auf der Günne, J.; Holthausen, M. C.; Schneider, S. *ACS Catal.* **2015**, *5*, 7214-7217.

(14) (a) Paul, A.; Musgrave, C. B. *Angew. Chem. Int. Ed.* **2007**, *46*, 8153-8156. (b) St. John, A.; Goldberg, K. I.; Heinekey, D. M. *Top. Organomet. Chem.* **2013**, *40*, 271−288.

(15) Esteruelas, M. A.; López, A. M.; Mora, M.; Oñate, E. *ACS Catal.* **2015**, *5*, 187-191.

(16) (a) Esteruelas, M. A.; Oliván, M.; Vélez, A. *Inorg. Chem.* **2013**, *52*, 5339-5349. (b) Haibach, M. C.; Wang, D. Y.; Emge, T. J.; Krogh-Jespersen, K.; Goldman, A. S. *Chem. Sci.* **2013**, *4*, 3683-3692.

(17) Esteruelas, M. A.; Oliván, M.; Vélez, A. *Inorg. Chem.* **2013**, *52*, 12108-12119.

(18) Esteruelas, M. A.; Oliván, M.; Vélez, A. *Organometallics* **2015**, *34*, 1911-1924.

(19) Esteruelas, M. A.; Oliván, M.; Vélez, A. *J. Am. Chem. Soc.* **2015**, *137*, 12321-12329.

(20) Multiple Quantum Magic Angle Spinning is a 2D experiment that allows to reveal subspecies contained under the same chemical shift in the 1D experiment. The signal splitting in the indirect dimension is due to the different Second Order Quadrupolar Effect, which is characteristic of quadrupolar nuclei such as ^{11}B (I = 3/2). See: (a) Frydman, L.; Harwood, J. S. *J. Am. Chem. Soc*. **1995**, *117*, 5367−5368. (b) Amoureux, J.-P.; Fernandez, C.; Steuernagel, S. *J. Mag. Reson.* **1996**, *A123*, 116-118.

(21) (a) Sewell, L. J.; Lloyd-Jones, G. C.; Weller, A. S. *J. Am. Chem. Soc.* **2012**, *134*, 3598-3610. (b) Robertson, A. P. M.; Leitao, E. M.; Jurca, T.; Haddow, M. F.; Helten, H.; Lloyd-Jones, G. C.; Manners, I. *J. Am. Chem. Soc.* **2013**, *135*, 12670-12683.

(22) Bluhm, M. E.; Bradley, M. G.; Butterich, R., III; Kusari, U.; Sneddon, L. G. *J. Am. Chem. Soc.* **2006**, *128*, 7748-7749.

(23) (a) Malakar, T.; Roy, L.; Paul, A. *Chem. Eur. J.* **2013**, *19*, 5812-5817. (b) Bhunya, S.; Malakar, T.; Paul, A. *Chem. Commun.* **2014**, *50*, 5919-5922. (c) Bhunya, S.; Zimmerman, P. M.; Paul. A. *ACS Catal.* **2015**, *5*, 3478-3493.

(24) An $OsH_6\{xant(P^iPr_2)_2\}$ complex containing a bidentate phosphine has been previously isolated and fully characterized: Alós, J.; Bolaño, T.; Esteruelas, M. A.; Oliván, M.; Oñate, E.; Valencia, M. *Inorg. Chem.* **2013**, *52*, 6199-6213.

(25) Esteruelas, M. A.; López, A. M.; Oliván, M. *Chem. Rev.*, DOI: 10.10/21/acs.chemrev.6b00080.

(26) Pathways with the diphosphine acting as a pincer and pathways involving an initial N-H bond activation of ammonia-borane were also taken into account. However, all of them are higher in energy.

(27) Kawano, Y.; Yamaguchi, K.; Miyake, S.; Kakizawa, T.; Shimoi, M. *Chem. Eur. J.* **2007**, *13*, 6920-6931.

(28) See for example: (a) Johnson, H. C.; McMullin, C. L.; Pike, S. D.; Macgregor, S. A.; Weller, A. S. *Angew. Chem. Int. Ed.* **2013**, *52*, 9776-9780. (b) Johnson, H. C.; Leitao, E. M.; Whittell, G. R.; Manners, I.; Lloyd-Jones, G. C.; Weller, A. S. *J. Am. Chem. Soc.* **2014**, *136*, 9078-9093.

(29) This compound exists as two conformers (**5a** and **5b**) associated to the rotation of BH_2NH_3 around the Rh-B bond.

(30) This relatively high value may be a consequence of the fact that the calculations reproduce well the dipolar moment of the solvent (tetrahydrofuran), but do not reproduce its coordination power and ability to form hydrogen bonds. In this sense, it should be mentioned that when the calculations are performed under vacuum the barrier decreases to 19.1 $kcal{\cdot}mol^{-1}$.

(31) Staubitz, A.; Sloan, M. E.; Robertson, A. P. M.; Friedrich, A.; Schneider, S.; Gates, P. J.; Schmedt auf der Günne, J.; Manners, I. *J. Am. Chem. Soc.* **2010,** *132*, 13332-13345.

(32) Zhao, Y.; Truhlar, D. G. *Theor. Chem. Acc.* **2008**, *120*, 215−241.

(33) Frisch, M. J.*, et al* Gaussian 09, Revision A.01, Gaussian, Inc., Wallingford CT, 2009.

(34) Marenich, A. V.; Cramer, C. J.; Truhlar, D. G. *J. Phys. Chem. B* **2009**, *113*, 6378−6396.

(35) Andrae, D.; Häußermann, U. M.; Dolg, M.; Stoll, H.; Preuß, H. *Theor. Chim. Acta* **1990**, *77*, 123−141.

DFT calculations suggest the existence of a monohydride pathway for the ammonia-borane dehydrogenation, which involves a stepwise hydrogen transfer from the substrate to the metal center, and produces a change of two units in the metal oxidation state.